Adsorption of Methylene Blue using the Biosorbent of Coconut Fiber Activated by Nitric Acid

Anselmus Boy Baunsele[1]*, Aloisius Masan Kopon[1], Erly Grizca Boelan[1], Maria Aloisia Uron Leba[1], Faderina Komisia[1], Maria Benedikta Tukan[1], Maximus Markus Taek[2], Gerardus Diri Tukan[2], Hildegardis Missa[3], Dwi Siswanta[4], Johnson Nune Naat[5], Rahayu[6]

[1]Chemical Education Study Program, Faculty of Teacher Training and Education, Widya Mandira Catholic University, Kupang, East Nusa Tenggara, Indonesia
[2]Chemistry Study Program, Faculty of Mathematics and Natural Sciences, Widya Mandira Catholic University, Kupang, East Nusa Tenggara, Indonesia
[3]Biology Education Study Program, Faculty of Teacher Training and Education, Widya Mandira Catholic University, Kupang, East Nusa Tenggara, Indonesia
[4]Department of Chemistry, Faculty of Mathematics and Natural Sciences, Gadjah Mada University, Yogyakarta, Indonesia
[5]Chemical Education Study Program, Faculty of Teacher Training and Education, Nusa Cendana University, Kupang, East Nusa Tenggara, Indonesia
[6]Department of Chemistry, Faculty of Mathematics and Natural Sciences, University of Pattimura, Ambon, Indonesia

*Corresponding author email: boybaunsele@gmail.com

ABSTRACT. The textile industry in the world keeps increasing, but it harms environmental pollution caused by textile dye waste. Synthetic dyes contain carcinogenic and mutagenic ingredients that can demage the environment and aquatic biota. The alternative to handling dye pollution with a low-cost method is adsorption using nitric acid-activated coconut fiber. Coconut fiber was an abundant agricultural waste and economical, and it had an active site that contained many compounds such as cellulose, lignin, pyroligneous acid, and tannin molecules. This study used the UV-Vis Spectrophotometer analysis method to determine the effect of pH, contact time, and coconut fiber on the adsorption capacity of methylene blue. The result showed that the optimal conditions for adsorption were a pH of 5, a contact time of 75 minutes, and a percentage adsorption of the variation of contact time of 99.628%. The adsorption study was according to a pseudo-second-order reaction with a constant reaction rate of 0.050 g mg^{-1} minute^{-1}. The maximum adsorption capacity was 2 mg g^{-1}, with the percentage of methylene blue adsorbed at 99.84%. Adsorption occurs chemically with an energy of 35.4 kJ mol^{-1}, so it can be determined that it occurs with a monolayer mechanism.

Keywords: Adsorption, biosorbent, isothermal, kinetic, methylene blue

INTRODUCTION

The population increase caused various environmental problems, namely the existence of organic and inorganic contaminants that are discharged into nature (El-Bindary et al., 2022). The industrial sector is beneficial in complying with human needs. Industrial waste consists of heavy metals or dyes. Heavy metals can accumulate in the body and cause various diseases (Yang et al., 2016). Besides heavy metals, dye is the material that is used for industrial processes. Dyes are indispensable materials for the textile, leather tanning, and paper dyeing industries (Chen et al., 2017). However, dyes are one of the pollutants produced by textile industry activities. About 10–15% of unused dyes in the textile industry are discharged into the environment (Purnaningtyas et al., 2020). Dyes in the textile

industry are mutagenic and carcinogenic, reducing water quality and threatening the survival of humans and animals (Xu et al., 2020). Their persistence stems from the challenging degradation process, as they resist aerobic decomposition, sunlight exposure, and the effects of oxidizing agents (Rangabhashiyam et al., 2013). One of the most used dyes in the textile industry is methylene blue. This dye can cause some effects on human health, including an increase in the heart rate, nausea, the formation of granules in red blood cells, and a lack of oxygen levels in the blood (Hashemian et al., 2013), vomiting, severe seizures, cyanosis, jaundice, quadriplegia, and necrosis in humans (Esmaeili and Foroutan, 2019) and irritation of the digestive tract (Ahmad et al., 2019). Besides this, dyes can reduce the amount of oxygen in water (Lellis et al., 2019), protect sunlight transmission, and

reduce biological metabolic processes, which cause the aquatic biota to degrade (Adegoke and Bello, 2015). Methylene blue (MB), one of the cationic dyes, has been widely used in textile companies and has carcinogenic properties, so it must be taken seriously. Because of its widespread application in the textile sector, methylene blue, a usual cationic dye, was the model chemical substance for adsorption (Alsubaie et al., 2021). This article is to show further research regarding the treatment of methylene blue.

Many researchers have developed methods for reducing dye components as environmental pollution. Some commonly used methods include coagulants based on plants (Jorge et al., 2022), ion exchange (Zhang et al., 2015), photodegradation (Kumar et al., 2019), and electrochemical oxidation techniques (Jawad and Najim, 2018). Another method that is often used is electroflotation. This process utilizes an electrode system to generate fine bubbles, facilitating the flotation of microalga particulates to the surface. It aims to purify water that is polluted by dyes (Talaiekhozani et al., 2020). Another method is the photocatalytic method. This method was developed to reduce water contamination by dyes utilizing a TiO_2-Zeolite catalyst. Mechanism occurs through dyes' degradation (Zuo et al., 2014). The biodegradation of methylene blue can be carried out using bacteria isolated from contaminated soil (Ariffin and Anuar, 2022). Although some of the presented methods successfully eliminate methylene blue, they still come with a price tag and take a while to complete (Ahmad et al., 2020). In addition, the adsorption method is considered the cheapest (Pathania et al., 2017). Adsorption as a simple separation method with high efficiency has always been regarded as an effective means; moreover, it has the advantage of flexibility in operation (Çetintaş, 2021). The effectiveness of adsorption arises from the tendency of the adsorbate to be adsorbed to the adsorbent surface, both chemically and physically (Fatah et al., 2022). Various natural materials are used for the adsorption of methylene blue including rice husk and sunflower seed coats (Adegoke and Bello, 2015),clove leaves (Kusuma et al., 2023), macroalgae (Daneshvar et al., 2017), papaya bark fiber (Nipa et al., 2023), fig tree bark (Pathania et al., 2017), teak leaves (Mishra et al., 2015), mytella falcata (Silva et al., 2017), raphia fibers (Staroń et al., 2019), banana pith (Hasan et al., 2020), fava bean peel waste (Bayomie et al., 2020), sawdust of sour lemon, date palm, and eucalyptus (Esmaeili and Foroutan, 2019), palm fruit coir (Ninu and Baunsele, 2023); (Banamtuan et al., 2023) and coconut fiber (Baunsele and Missa, 2020) (Baunsele and Missa, 2021) (Baunsele et al., 2023).

Agricultural waste is abundant, so various researchers can use it as an adsorbent to improve environmental quality (Karić et al., 2022). Plants can

be used as metal nanoparticle production agents and dye adsorbents (Nandhini et al., 2019). One of the many natural ingredients that have the potential to be used is coconut. Coconut plants have many functions for humans. In pharmaceuticals, coconut water can increase body immunity (Hasti et al., 2021) and coconut coir ethanol extract has been used as a bacterial growth inhibitor (Wulandari et al., 2019). In agriculture, coconut husk waste is used for local microorganisms fermented solutions (Dharma et al., 2018). For adsorbents, coconut dregs are heavy metal adsorbents (Kamari et al., 2014). Utilizing various coconut by-products, researchers have explored their potential as effective adsorbents for methylene blue: coconut bunch waste (Cocos nucifera) (Hameed et al., 2008), coconut coir dust (Etim et al., 2016), and activated carbon derived from coconut shells (Khuluk et al., 2019).

This study used nitric acid-activated coconut coir as a methylene blue adsorbent. Chemical activation of the adsorbent is carried out to obtain better adsorption results than the untreated adsorbent. This research continues previous research that only carried out methylene blue adsorption without treatment on coconut fiber (Baunsele and Missa, 2021, 2020). Chemical activation can take the form of acid or base activation. This process causes changes on the surface of the adsorbent, altering the form of adsorbent pores to become increasingly open and enhancing opportunities for the adsorption process to occur without any inhibition (Doondani et al., 2022). In previous research, activation of coconut coir using NaOH was carried out and then used for methylene blue adsorption (Baunsele et al., 2022).

Furthermore, activation can be done with an acid solution. The activation process using hydrochloric acid can reduce impurities in the adsorbent to increase the adsorption capacity. Impurities can close the active site on the adsorbent to protect the adsorbate and allow it to interact appropriately with the adsorbent (El-Bery et al., 2022). The research aimed to investigate the impact of pH and contact time on the adsorption capacity of nitric acid-activated coconut fiber (CFAA) for methylene blue (MB). This paper reports the kinetics and isothermal study of methylene blue adsorption by nitric acid-activated coconut fiber.

EXPERIMENTAL SECTION
Materials and Instrumentation

The materials used were coconut fiber and aquadest. The reagents used in this research include methylene blue (Merck), HNO_3 (Merck, 65%), NaOH (Merck, 99%), and HCl (Merck, 37%). Sample characterization was using UV-Vis (*Thermos Scientific*) in the Chemical Laboratory of Mathematics and Natural Sciences Faculty of Widya Mandira Catholic University in the Kupang City of Indonesia,

Fourier Transform Infrared Spectroscopy (Shimadzu IR Prestige 21) and Scanning Electron Microscope (JSM-6510LA) analyzed in Centre Research and Testing Laboratory of Gadjah Mada University in Yogyakarta City of Indonesia.

Adsorbent Preparation

The coconut coir sample was separated from the fruit skin and then pulverized using a mortar and sieved with a mesh size of 100 Mesh. The biosorbent was then immersed in 0.4 M concentrated nitric acid for 2 hours. After the biosorbent was activated, it was washed with distilled water to obtain a pH of 7. The sample was then dried at 70 °C for 4 hours and used as an adsorbent for methylene blue. The acid-activated biosorbent is then called CFAA. The CFAA was characterized using Fourier Transform Infrared Spectroscopy (FTIR) and Scanning Electron microscopy (SEM). The research procedure is shown in **Figure 1**.

The zero-charge point (pzc) of the biosorbent was determined using the pH change value at 24 hours. The pH point of zero charge (pH$_{pzc}$) can be determined by adding 20 mL of 0.1 M NaCl solution of a known initial pH to several flasks and then modifying the pH of the solution with 0.1 M NaOH or 0.1 M HCl to make it between 1 and 8. Next, 0.1 g biosorbent is added to each flask. It is then agitated at 100 rpm for 24 hours, and the pH of each solution is tested once more. pH$_i$ refers to the initial pH, while pH$_f$ refers to the final pH (Bello et al., 2019).

Determination of Calibration Curve

Methylene blue stock solution of 100 ppm was prepared by dissolving 100 mg of methylene blue into 1000 mL of distilled water. The MB 100 ppm standard solution was diluted to 5 ppm, and then the largest absorbance was determined with a wavelength variation of 500–700 nm. The wavelength with the largest absorbance will be used to analyze the adsorption process further. The calibration curve was obtained by diluting the MB stock solution into a concentrated solution of 0, 2.5, 5, 7.5, and 10 ppm and then measuring the absorbance using a UV-Vis spectrophotometer. The absorbance data obtained is then used to determine the linear equation.
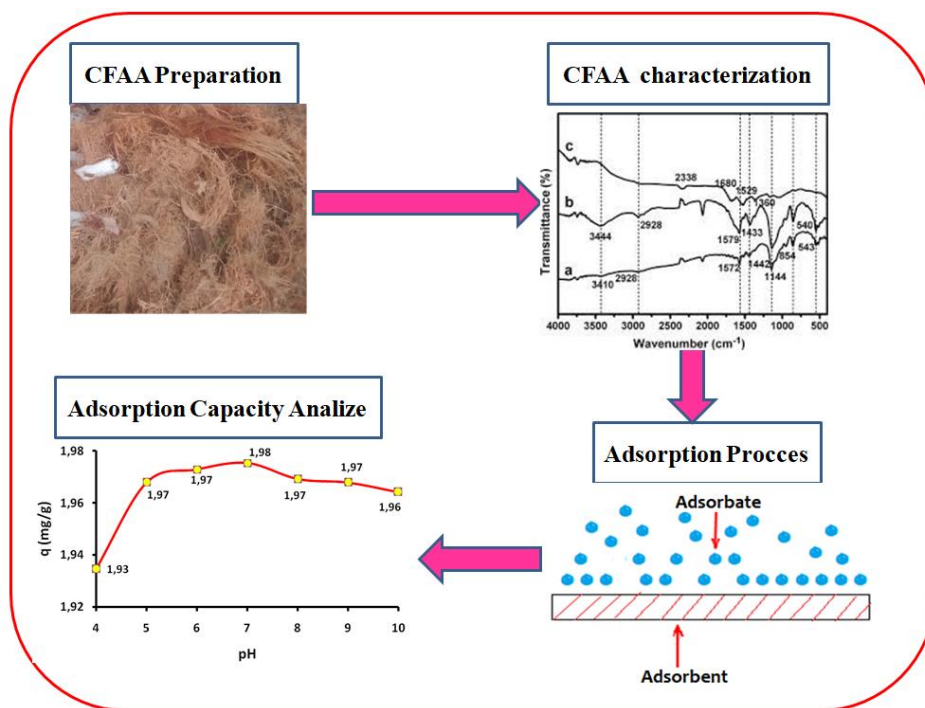
Figure 1. Research procedure

Table 1. Mathematical model used to study MB adsorption kinetics using CFAA

Kinetics Model	Linear shape	Graph plot	References
PFO	$ln(qe - qt) = ln\,qe - \dfrac{kt}{2,303}$	*ln (qe – qt) vs t*	(Handayani et al., 2023)
PSO	$\dfrac{1}{qt} = \dfrac{1}{K_2 qe^2} + \dfrac{t}{qe}$	$\dfrac{t}{qt}\,vst$	(Sharma et al., 2023)
Elovich	$qt = \left(\dfrac{1}{ß}\right)ln(\alpha ß) + \left(\dfrac{1}{ß}\right)ln\,t$	*qt vs ln t*	(Ganguly et al., 2020)

Table 2. Mathematical models of the adsorption isotherm

Isothermal model	Linear regression	Graph Plot	Reference
Langmuir	$\dfrac{1}{qe} = \dfrac{1}{Qo} + \dfrac{1}{KlQoCe}$	$\dfrac{1}{qe}\,vs\,\dfrac{1}{Ce}$	(Neolaka et al., 2020)
Freundlich	$log\,qe = log\,Kf + \dfrac{1}{n}log\,Ce$	$Log\,qe\,vs\,log\,Ce$	(Neolaka et al., 2020)
Temkin	$qe = \text{ß}\,ln\,K_T + B\,ln\,Ce$	$ln\,Ce\,vs\,qe$	(Ahmad et al., 2019)
Harkin-Jura	$\dfrac{1}{qe^2} = \dfrac{B}{A} - \left(\dfrac{1}{A}\right)log\,Ce$	$\dfrac{1}{qe^2}\,vs\,log\,Ce$	(Ayawei et al., 2017)
Redelich-Peterson	$ln\,\dfrac{Ce}{qe} = \text{ß}\,ln\,Ce - ln\,A$	$ln\,\dfrac{Ce}{qe}\,vs\,ln\,Ce$	(Ayawei et al., 2017)
Jovanovic	$ln\,qe = ln\,q_{max} - K_j Ce$	$ln\,qe\,vs\,Ce$	(Ayawei et al., 2017)

The Effect of pH

A total of six containers were prepared and entered at 20 mL MB 10 ppm. The pH of each container is adjusted from 4 to 9. Then 0.01 gram of biosorbent was added to each container and shaken for 75 minutes. The mixture was then filtered to separate the residue and filtrate. The filtrate was analyzed using UV-Visto determine the amount of adsorbed methylene blue, and then the pH of the MB solution with the largest adsorption was obtained. The percentage adsorption of MB was calculated using Equation 1. The adsorption capacity was calculated using Equation 2.

$$\%\,of\,adsorption = \frac{Co - Ce}{Co}\,x\,100\% \qquad (1)$$

$$q = \frac{(Co - Ce)v}{m} \qquad (2)$$

Co is the initial concentration before adsorption, and Ce is the concentration after adsorption. While v represents the volume of MB and m represents the mass of CFAA. q is the adsorption capacity of the adsorbate by the adsorbent (mg/g) (Parushuram et al., 2022).

Adsorption Kinetic

A 20 mL MB solution (10 ppm) was made at optimum pH and interacted with a 0.1 gram CFAA adsorbent. The containers were then shaken with various contact times of 5, 10, 20, 40, 50, 75, 90, and 120 minutes, respectively. After the adsorption process, the solution is filtered using filter paper, and the absorbance is measured using a UV-Vis spectrophotometer. By using the calibration curve, the solution concentration can be generated, and equation 1 can be used to determine the percentage of adsorption. Three studied kinetic models are presented in **Table 1**, and the corresponding adsorption kinetics are those with an R-value close to 1, which is the kinetic adsorption of MB by CFAA.

Adsorption Isotherm

The adsorption isotherm was carried out by varying the concentration of 20 mL of MB from 5 to 75 ppm in the Erlenmeyer flask. The CFAA, about 0.1 g, was added to the solution and stirred for optimum time. The MB concentration was measured using a UV-Vis spectrophotometer. The isothermal adsorption of Langmuir, Freundlich, Temkin, Harkin-Jura, Redelich-Peterson, and Jovanovic on the CFAA was investigated, as shown in **Table 2**. The R^2 value of each model closest to 1 is the isotherm model of MB adsorption.

RESULTS AND DISCUSSION
Biosorbent Preparation

The coconut coir sample is cleaned and separated from the fruit skin, then the fiber is crushed using a mortar. Furthermore, the coconut fiber was then pulverized to a size of 100 mesh. Refining coconut coir is to obtain a smaller and more homogeneous sample size so that the surface area of the coconut coir sample will increase (Neolaka et al., 2023). Coconut coir powder was then activated using 0.4 M nitric acid for 2 hours of immersion. Acid activation can be utilized to increase the adsorption capacity of dyes because it has been reported to increase the pore size of the adsorbent (Iriarte-Velasco et al., 2016). Activated coconut coir is washed with water until the pH becomes neutral and then dried. It is called coconut fiber acid activated (CFAA).

FTIR Characterization

The characterization of the CFAA biosorbent was carried out using the FTIR and SEM instruments. The FTIR was employed to determine the functional groups' content in CFAA and what functional groups might bind to MB. Figure 2 shows the FTIR spectra for pure CF, CFAA, and CFAA-MB. In **Figure 2**, the C–H alkane bond is described at a 2916 cm^{-1} peak to 2919 cm^{-1} after acid activation, indicating cellulose, hemicellulose, and lignin molecules. These peaks of wave numbers 3296, 3341, and 3449 cm^{-1} indicated the presence of O–H alcohols of phenol functional groups, which also describe the existence of cellulose (Salazar-Rabago et al., 2017).

At the peak of 3341 cm^{-1}, there is a stretching vibration between O—H and the hydrogen atoms with other atoms by hydrogen bonds, which causes the vibration to be weak. Before activation, O—H showed a peak at 3296 cm^{-1}, but after acid activation, the peak shifts to 3341 cm^{-1}, and when adsorption of MB occurs, the peak changes to 3449 cm^{-1} with a weak intensity. It showed that

the acid and MB bound to the surface of the adsorbent will reduce the bond vibration. In addition, the sharp peak with a wave number of 1609, 1601, and 1630 cm^{-1} indicates the presence of a C=C alkene bond in cellulose (Markovi et al., 2015). After the activation and adsorption processes, the peak becomes dull due to the weak vibration intensity. The two peaks of 1107 and 1107 cm^{-1} represent stretching vibrations of the C-O of the alcohol, ester, and carboxylic acids (Etim et al., 2016). Two peaks at 2725 and 2729 cm^{-1} can be attributed to cellulose's bending fibration of the C–H bonds of the –CH$_3$ groups. Some functional groups observed in CFAA biosorbents are similar to some of the research results in **Table 3**.

Surface Morphology of CFAA

The surface morphology of CFAA was obtained using SEM and SEM-EDX. **Figure 3** shows the SEM images of the morphology of CFAA before and after the addition of MB. The surface morphology is uniform and smooth, even before adsorbing MB. No other components are bound to the biosorbent surface. No other components are bound to the biosorbent surface. It can be seen that the CFAA surface has a lot of pores, and that feature can increase the adsorption capacity (Nipa et al., 2023). After the sorption process, substantial changes in the CFAA surface were observed, due to the impregnation of MB on the surface of the biosorbent. Furthermore, the surface of CFAA was seen as rough and irregular. These characteristics indicated an interaction between MB and the functional groups of CFAA. The CFAA surface was covered by a crude polymer. Based on **Figure 4** as an image of EDX analysis, CFAA contains elements such as C (49,93%), N (14,37%), and O (35,70). These elements are evenly distributed on the surface of the absorbent. Observed carbon and oxygen elements support the FTIR data showing C—O bonds in alcohol, ester, and carboxylic acids. Nitrogen indicates the presence of MB, which is adsorbed on CFAA, because in MB there is an azo bond (—N=N—), which acts as a chromophore in molecular composition (Kusuma et al., 2023).

Table 3. FTIR data of several biosorbent

Functional groups	Wavenumber (cm^{-1})	Biosorbent
C—H; O—H; C—C; C=O	935; 2900 and 1430; 3500-3000; 1619	Avocado seeds (Díaz-muñoz et al., 2016)
C—H; O—H; C=C; C—O	2939,52; 3296.35; 1608,63 and 817,72; 1267,23 and 1060,85	Coconut fiber (Baunsele and Missa, 2021)
C—H; O—H; C—C; C—O	1459 dan 1377; 3370; 2923 and 2854; 1744 and 1711	Coconut pulp (Kamari et al., 2014)
C—H; O—H; C—C; C=O; C—O	2918.53; 3433; 1629.99; 1431.02; 1162.2	Figs (Pathania et al., 2017)
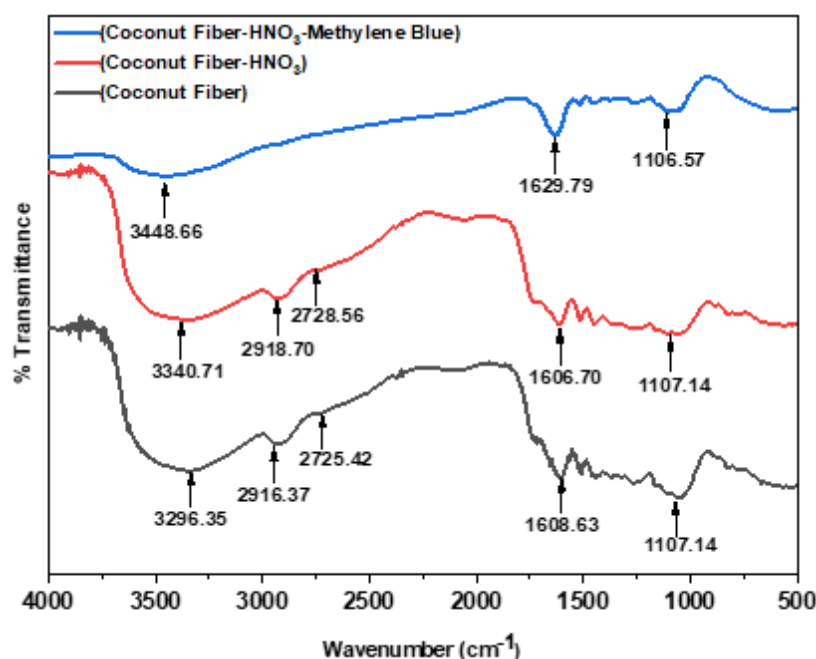
Figure 2. FTIR spectra of pure CF, CFAA, and CFAA-MB
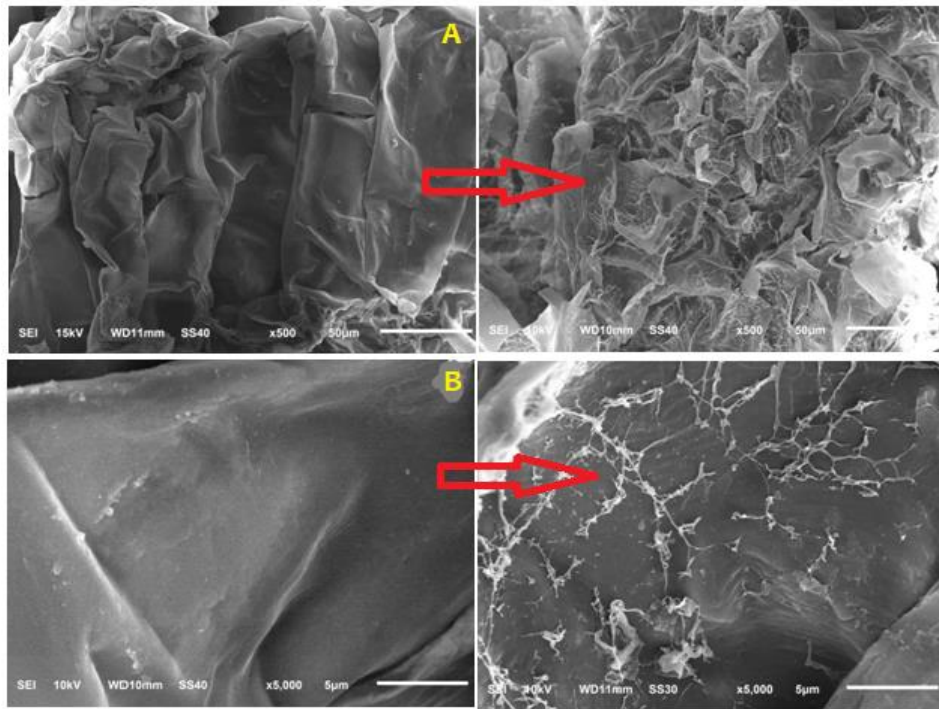
Figure 3. SEM analyzed before and after adsorption for magnifications of (**A**) 500× and (**B**) 5000×

Element	Wt %	At %
CK	43.71	49.93
NK	14.67	14.37
OK	41.62	35.70
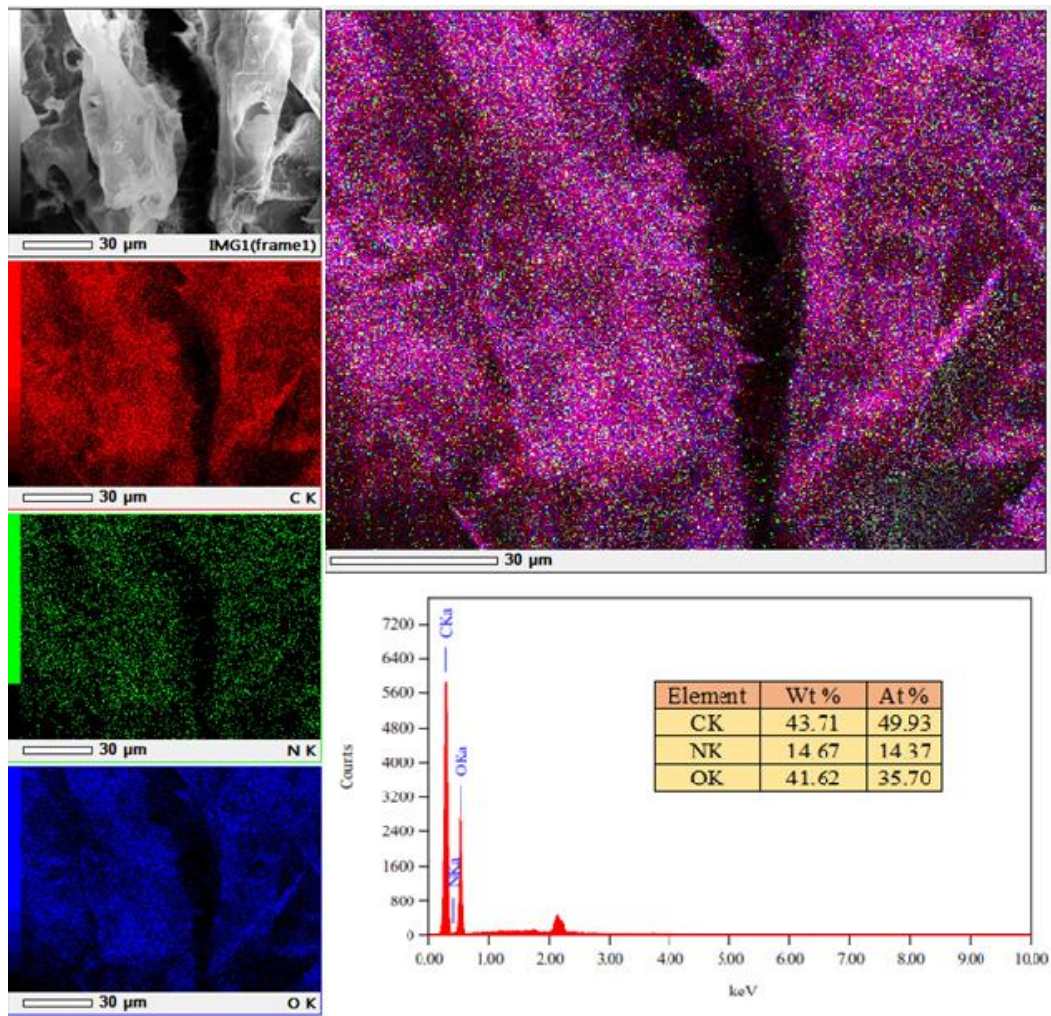
Figure 4. EDX Analysis

pH and point of zero charge pH (pH$_{pzc}$) determination

The pH point of zero charge (pH$_{pzc}$) was found to investigate the properties of the CFAA biosorbent. This adsorbent's properties aim to identify the pH range in which it interacts with MB. The salt addition method can be used to find pH$_{pzc}$. The pH$_{pzc}$ of CFAA shown in **Figure 5**, is 6. This result indicates that the adsorbent's surface is dominated by positive charges at pH values below pH$_{pzc}$ (6) and by negative charges at pH values above pH$_{pzc}$ on the surface of CFAA. This pH$_{pzc}$ is the pH value at which the positive and negative surface charges associated with protonation/deprotonation equilibrium are balanced in the presence of a nonreactive electrolyte (Al-Maliky et al., 2021).

Calibration Curve

The methylene blue was concentrated to 100 ppm as a standard solution, then diluted and used as a test solution. The determination of the maximum wavelength aims to determine the highest absorbance value of the MB test solution. Based on Lamber-Beer's Law, absorbance is directly proportional to concentration, meaning that if the absorbance increases, the concentration of the adsorbed analyte also increases (El-Bery et al., 2022). If the measurement is carried out on a solution with a constant concentration and the absorption wavelength is varied, the greatest absorbance can be obtained at the maximum wavelength or lambda. The maximum lambda (λ max) used in this study was obtained from the results of previous studies at a wavelength of 665 nm (Baunsele and Missa, 2020). The maximum wavelength is also the same as that found in research on the adsorption of methylene blue using reed cellulose (Huda and Yulitaningtyas, 2018). It is known that the complementary color of blue is in the range of wavelengths 650–670 nm, so there are similarities with several studies that have varied the maximum absorption of methylene blue, such as 662 nm (Dwiasi et al., 2018), 665 nm (Baunsele et al., 2022) and 664 nm (Handayani et al., 2023).

The λ max data obtained was then used to determine the standard curve of methylene blue absorbance. The standard curve data shown in **Figure 6** was obtained from plot data of absorbance versus adsorbate concentration (0, 2.5, 5, 7.5, and 10 ppm). Based on **Figure 6**, we can see that the regression equation is y = 0.162x + 0.002, and R^2 is 0.999. The correlation coefficient of this study shows the linearity of the plotted data. It is known that the value of the correlation coefficient is positive, so there is a directly proportional relationship between absorbance and concentration. The regression equation obtained in **Figure 6** is used to determine the adsorption capacity in optimum conditions, such as pH, concentration, and contact time.
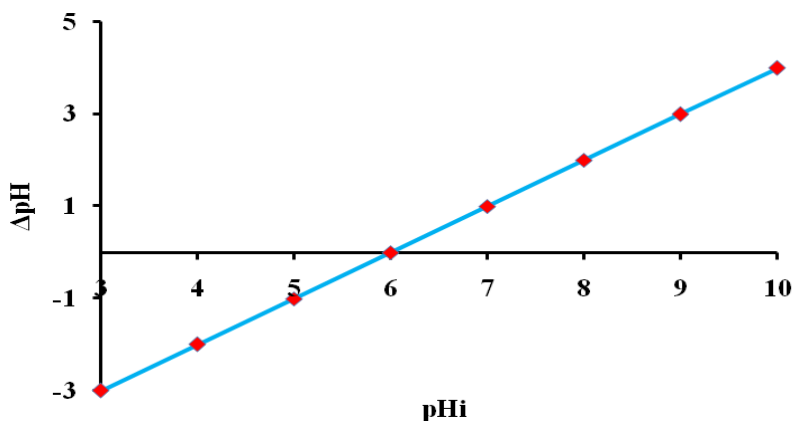
Figure 5. pH$_{pzc}$ of CFAA
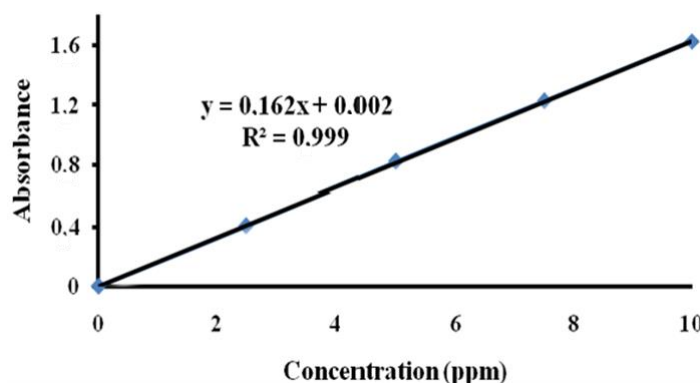
Figure 6. Standard curve of MB adsorption
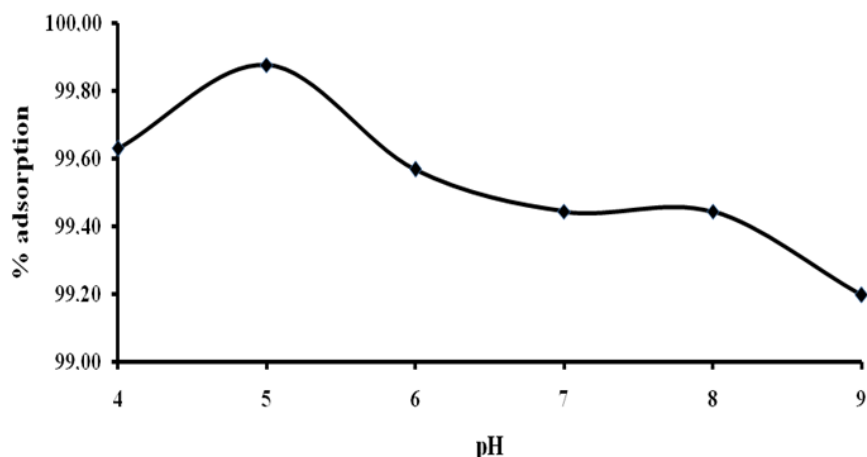
Figure 7. Effect pH of MB adsorption

Effect of pH

Optimum pH values were obtained by reacting methylene blue solutions at various pH levels from 4 to 9 with CFAA. The adsorption capacity is affected by the solution pH presented in **Figure 7**. Based on **Figure 7**, it is clear that there is an increase in adsorption capacity from pH 4 to pH 5. When the pH of the MB solution is 4, the H$^+$ ion will protonate the methylene blue so that there is a competition between the positive partial of MB and the hydrogen ion to interact with the active site of CFAA. As a result of this mechanism, the active group of cellulose on the surface of CFAA will be covered by H$^+$ ions, so there will be repulsion between CFAA and MB, which causes the percentage of MB adsorption to be low. Adsorption capacity at pH 5 was the best condition, with the largest adsorption percentage of 99.87%, due to the availability of active sites on CFAA and protonated MB, which increased the amount of MB absorbed on CFAA. The maximum adsorption capacity with a pH of 5 was 19.79 mg g^{-1}. When pH is above 5, MB can form ionic zwitters and dipoles, so there is a possibility of forming dimers of the MB molecule. The size of the zwitter ion or dimer molecule will be large so it will be difficult to enter the pores of the CFAA surface (Sulaeman et al., 2023). Besides that, the adsorption capacity at a pH above 5 is very small because, in these conditions, the OH$^-$ ion will cause an electrostatic interaction with the positive charge on the MB and can protect the interaction between the MB and CFAA. That was because the surface of the biosorbent became negative (Doondani et al., 2022). Moreover, the CFAA surface was covered by OH$^-$ ions, which caused steric hydrogenation between the adsorbate and the adsorbent.

Adsorption kinetic

The maximum contact time is the contact time for the largest adsorption capacity of MB on CFAA. **Figure 8** shows that the optimum contact time occurs at 75 minutes. From 5 to 10 minutes, there was a significant increase in adsorption capacity, which became constant after 75 to 120 minutes. This stability in adsorption is due to the fact that during this period, the pores and the active site of the CFAA were vacant, allowing the MB to be adsorbed to CFAA. After 75 minutes, it is known that there is equilibrium adsorption, so no more MB is bound to the CFAA active site but diffused into the CFAA surface (Umaningrum et al., 2023).The decrease in adsorption capacity was explained by the decrease of the active site on CFAA (Purnaningtyas et al., 2020). Adsorption capacity (qt) at 75 minutes to 120 minutes was the same, about 19.74 mg g^{-1} with a percentage of 99.628%.As demonstrated by earlier studies, which found that the adsorption capacity was only 99,14% (Baunsele and Missa, 2020), the results of this investigation demonstrate that CFAA has a higher adsorption capacity than coconut fiber without activation.

The mechanism of the adsorption process on the surface of the adsorbent is: (1) Adsorbate molecules are moving from the bulk solution to the adsorbent's surface, (2) diffusion to the surface of the adsorbent via the boundary layer, (3) adsorption at a site, and (4) internal adsorbent diffusion of intraparticle. As an outcome, adsorbate diffusion to the adsorbent surface increases as the adsorbate flows towards it (Geethamani et al., 2014).

One of the vital parameters in this study was the kinetic study of MB adsorption using CFAA. The determination of the kinetic reaction using three equations: pseudo-first order, pseudo-second order, and Elovich. The kinetic parameters obtained in **Table 4** are the results of the data plot curve for each kinetic model in **Table 1**. Based on **Table 4**, the correlation coefficients for PFO and Elovich kinetic models are smaller than the R^2 value of PSO. This correlation coefficient data explains the adsorption of methylene blue on CFAA according to pseudo-second order kinetics. **Figure 9A** shows an equilibrium concentration between the amount of adsorbate adhered to the surface of the adsorbent per minute. According to the PFO, the adsorption capacity was 9.08 mg g^{-1}, which means that 9.08 mg

of adsorbate can be absorbed to 1 g of adsorbent in the adsorption process. The rate constant in the pseudo-first-order kinetics assumed that every minute of the adsorption process was involved among 0.0004 parts of the total adsorbate. **Figure 9C** indicated that the constant of MB adsorption was 0.0505 g per mg absorbed. The initial adsorbate adsorption rate was 9.25 mg g^{-1} min^{-1}. Elovich assumed that the adsorbate would distribute to the CFAA surface with heterogeneous energy (Ebelegi et al., 2020). Based on **Figure 9B**, The R^2 value in the regression equation is 1, meaning there

is a relationship between the variable's t/qt and time. The reaction rate constant for the second-order pseudo is 0.050 g mg^{-1} $minute^{-1}$, which means that every 1 mg of adsorbent used for the adsorption process for one minute will absorb as much as 0.05 g of adsorbate, or in one minute using 1 mg of adsorbent, there will be a transfer of the MB liquid phase to the solid phase of CFAA of as much as 0.05 g. If the adsorption process is according to the PSO model, then the MB will be adsorbed at a limited rate, and the dominant sorption process is chemisorptions (Shakoor et al., 2018).
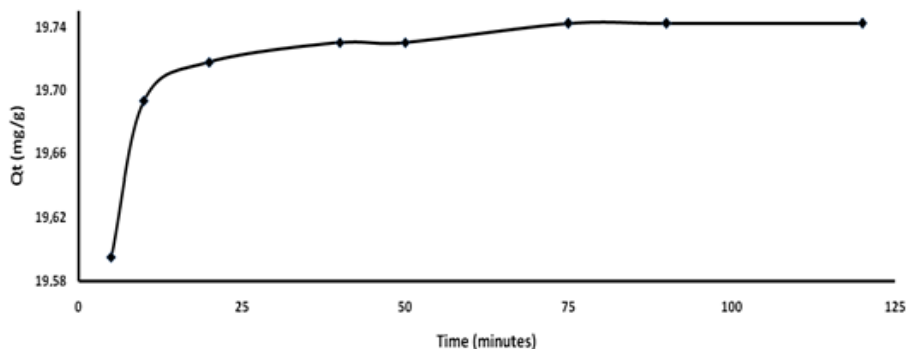
Figure 8. Effect of contact time on methylene blue adsorption

Table 4. Kinetic model constant parameters for MB adsorption unto CFAA.

Models	Kinetic parameters
PFO	K_1 (0.004 min^{-1})
	Qe (9.08 mg g^{-1})
	R^2 (0.768)
PSO	K_2 (2.5 min^{-1})
	Qe (20 mg g^{-1})
	R^2 (1)
Elovich	ß (0.0505 g mg^{-1})
	α (9.25 mg g^{-1} min^{-1})
	R^2 (0.778)
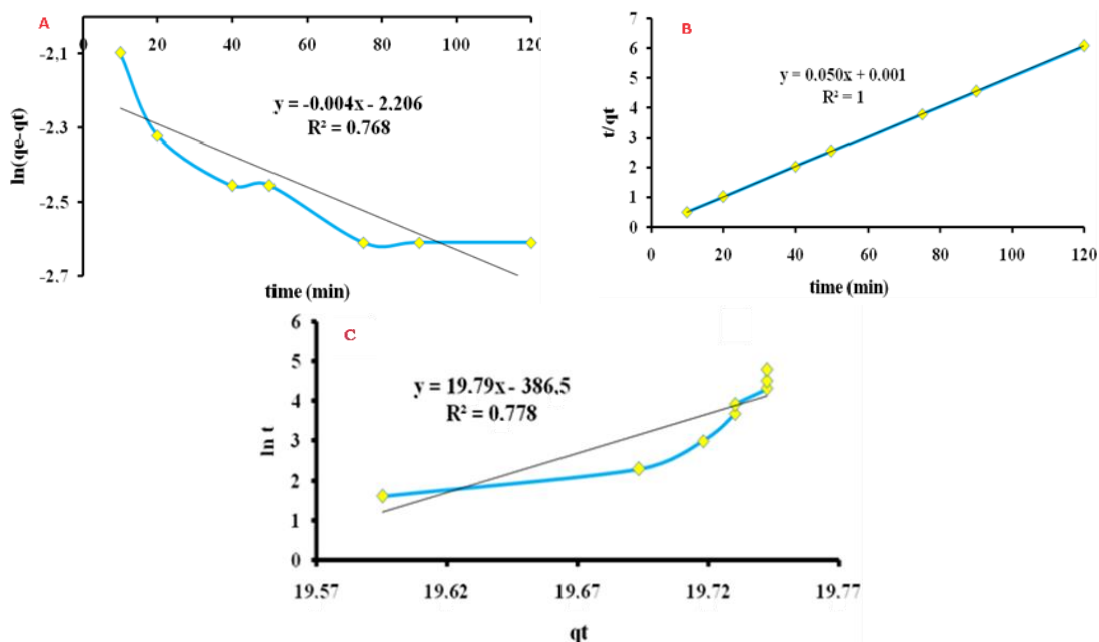
Figure 9. Kinetic model of MB adsorption: (**A**) Pseudo-first order, (**B**) Pseudo-second order, and (**C**) Elovich

Isothermal Adsorption of Methylene Blue

The adsorbate (MB) concentration effect was evaluated by varying the MB concentration in the range of 5 to 75 ppm. The adsorption process was carried out at pH 5 with a time adsorption of 75 minutes. Based on **Figure 10**, the maximum adsorption capacity of the adsorbate was 45 ppm with an adsorption percentage of 99.84%. We can assume that at concentrations of 5 to 20 ppm, the adsorption percentage increases due to the many active sites of CFAA that can promote the interaction with MB because the number of CFAA active sites is greater than the number of MB molecules. At concentrations above 45 ppm, the adsorption capacity decreased because the MB layer covered the active sites of CFAA, and further adsorption processes did not occur. Besides that, the decrease in capacity is caused by the fact that the number of active sites in the biosorbent is less than the number of adsorbate molecules (El-Bery et al., 2022).

The study of isothermal adsorption of MB onto CFAA was carried out using six isothermal models, as shown in **Table 2**. The correlation coefficient of each isothermal model was found a linear regression. The values of isothermal parameters are presented in **Table 5**, while the linear regression graph is shown in **Figure 11**. Based on **Table 5**, the isothermal model with an R^2 value close to 1 is the adsorption isothermal of MB into CFAA.

Table 5 presents the R^2 values of isothermal adsorption for Langmuir, Freundlich, Temkin, Harkin-Jura, Redelich-Peterson, and Jovacovic: 1; 0.957; 0.883; 0.714; 0.976; and 0.883, respectively. The regression correlation of Langmuir was 1, which indicated that the MB adsorption to the CFAA process
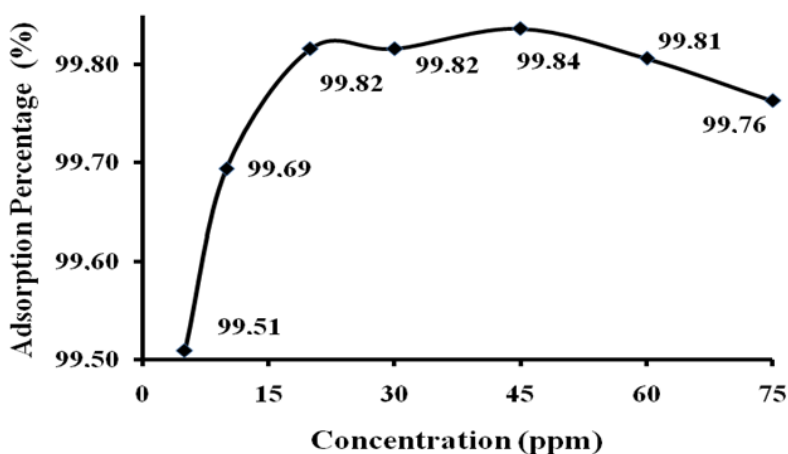
Figure 10. Effect of initial concentration of MB

Table 5. Isothermal adsorption parameters

Isotherm models	Parameter	value
Langmuir	Qmax (mg g^{-1})	2
	KL (L mol^{-1})	159925
	E (kJ mol^{-1})	35.392
	R^2	1
Freundlich	Kf (mg g^{-1})	2.302
	n	0.83
	R^2	0.957
Temkin	B	0.017
	A	0.68
	R^2	0.883
Harkin-Jura	A	0.01
	B	0.004
	R^2	0.714
Redelich-Peterson	Kr (L g^{-1})	108.202
	ß	20.01
	R^2	0.976
Jovanovic	Kj	24.84
	qmax (mg g^{-1})	1.01
	R^2	0.883
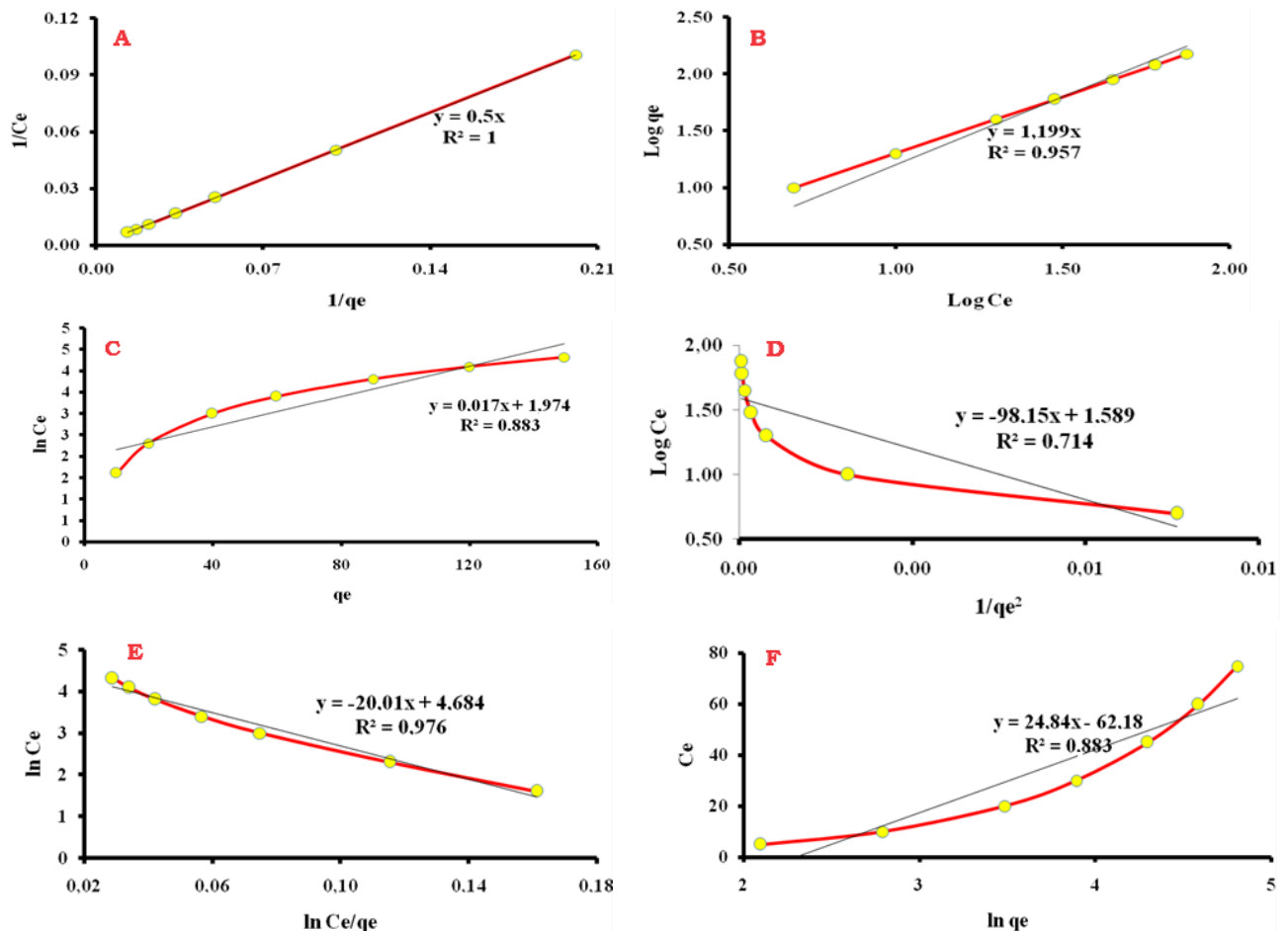
Figure 11. Isothermal adsorption plot graph: (**A**) Langmuir; (**B**) Freundlich; (**C**) Temkin; (**D**) Harkin-Jura; (**E**) Redelich-Peterson; and (**F**) Jovacovic

occurs in the Langmuir isotherm. Theoretically, Langmuir isotherms explain that the adsorption process causes a monolayer of adsorbate coverage on the adsorbent surface (Pathania et al., 2017), and each active site of the adsorbent surface can adsorb one molecule of adsorbate (El-Bery et al., 2022). This assumption is supported by the data in **Figure 8**, which shows that the adsorption equilibrium condition has reached 75 minutes. After more than 75 minutes, no adsorption or desorption has occurred. The qmax of MB adsorption was 2 mg g^{-1}, meaning that 1 g of CFAA can absorb as much as 2 mg of MB every 75 minutes of the adsorption process. The adsorption energy was 35.4kJ mol^{-1}, which indicates the adsorption process is chemisorption. Due to chemical adsorption, if the adsorption energy is greater than 8 kJ mol^{-1} and the physical adsorption is below 8 kJ mol^{-1} (El-Bindary et al., 2022).

CONCLUSIONS

The optimum conditions for methylene blue adsorption using coconut fiber nitric acid activation were obtained at pH 5 with a contact time of 75 minutes. The adsorption kinetics follow pseudo-second-order with an adsorption rate of 0.050 g mg^{-1}minute^{-1}. The isothermal adsorption follows the Langmuir equation, and the maximum adsorption amount is 2 mg g^{-1}. The adsorption process occurs according to chemisorption.

ACKNOWLEDGEMENTS

REFERENCES

Adegoke, K.A., & Bello, O.S. (2015). Dye sequestration using agricultural wastes as adsorbents. *Water Resources and Industry, 12,* 8–24. https://doi.org/10.1016/j.wri.2015.09.002

Ahmad, M.A., Ahmed, N.B., Adegoke, K.A., & Bello, O.S. (2019). Sorption studies of methyl red dye removal using lemon grass (*Cymbopogon citratus*). *Chemical Data Collections, 22,* 100249. https://doi.org/10.1016/j.cdc.2019.100249

Ariffin, F., & Anuar, N.EMC. (2022). Biodegradation of Methylene Blue By Bacteria Strains Isolated From Contaminated Soil. *Malaysian Applied*

Biology, 51, 25–35. https://doi.org/10. 55230/mabjournal.v51i3.2190

Ayawei, N., Ebelegi, A.N., & Wankasi, D. (2017). Modelling and Interpretation of Adsorption Isotherms. Journal of Chemistry, 2017,3039817. https://doi.org/10.1155/ 2017/3039817

Banamtuan, E. Theresia., Baunsele, A.B., & Kopon, A.M. (2023). Adsorption study of methylene blue utilizing palm fruit coil (Borassus flabellifer L.). Inovasi Teknik Kimia, 8, 108–116.

Baunsele, A.B., Boelan, E.G., Kopon, A.M., Rahayu, & Siswanta, D. (2022). Kinetic study of blue methylene adsorption using coconut husk base activated. Indonesian Journal of Chemical Research, 9, 129–136. https://doi.org/10. 30598//ijcr

Baunsele, A.B., Boelan, E.G., Kopon, A.M., Taek, M.M., Tukan, G.D., Missa, H., Kimia, S.P., Keguruan, F., Katolik, U., & Mandira, W. (2023). Utilization of coconut fiber NaOH-activated as blue methylene adsorbent. Kovalen: Jurnal Riset Kimia, 9, 43–54.

Baunsele, A.B., & Missa, H. (2021). Langmuir and freundlich equation test on methylene blue adsorption by using coconut fiber biosorbent. Walisongo Journal of Chemistry, 4, 131–138.

Baunsele, A.B., Missa, H. (2020). Kajian kinetika adsorpsi metilen biru menggunakan adsorben sabut kelapa. Akta Kimia Indonesia, 5, 76–85. https://doi.org/10.12962/j25493736.v5i2.7791

Bayomie, O.S., Kandeel, H., Shoeib, T., Yang, H., Youssef, N., & El-Sayed, M.M.H. (2020). Novel approach for effective removal of methylene blue dye from water using fava bean peel waste. Scientific Reports 10, 1–10. https://doi.org/10.1038/s41598-020-64727-5

Bello, O.S., Adegoke, K.A., Fagbenro, S.O., & Lameed, O.S. (2019). Functionalized coconut husks for rhodamine-B dye sequestration. Applied Water Science, 9, 189. https://doi.org/10.1007/s13201-019-1051-4

Çetintaş, S. (2021). An alternative application for reuse of leaching residues: Determination of adsorption behaviour for methylene blue and process optimization. Sustainable Chemistry and Pharmacy, 23, 100504. https://doi.org/ 10.1016/j.scp.2021.100504

Chen, C., Fu, Y., Yu, L.L., Li, J., &Li, D.Q. (2017). Removal of methylene blue by seed-watermelon pulp-based low-cost adsorbent: Study of adsorption isotherms and kinetic models. Journal of Dispersion Science and Technology, 38, 1142–1146. https://doi.org/ 10.1080/01932691.2016.1225263

Daneshvar, E., Vazirzadeh, A., Niazi, A., Sillanp, M., & Bhatnagar, A. (2017). A comparative study of methylene blue biosorption using different

modified brown, red and green macroalgae - effect of pretreatment. Chemical Engineering Journal, 307, 435–446. https://doi.org/10. 1016/j.cej.2016.08.093

Dharma, P., Suwastika, A., & Sutari, N. (2018). Study on the utilization of coconut coir waste as a solution for local microorganisms. Agroteknologi Tropika, 7, 200–210.

Díaz-muñoz, L.L., Bonilla-petriciolet, A., Reynel-ávila, H.E., Mendoza-castillo, D.I., México, T.N. De, & Aguascalientes, I.T. De. (2016). Sorption of heavy metal ions from aqueous solution using acid-treated avocado kernel seeds and its FTIR spectroscopy characterization. Journal of Molecular Liquids, 215, 555–564. https://doi.org/10.1016/j.molliq.2016.01.022

Doondani, P., Gomase, V., Saravanan, D., & Jugade, R.M. (2022). Chitosan coated cotton-straw-biochar as an admirable adsorbent for reactive red dye. Results in Engineering, 15, 100515. https://doi.org/10.1016/j.rineng. 2022.100515

Dwiasi, D.W., Setyaningtyas, T., & Riyani, K. (2018). Penurunan kadar metilen biru dalam limbah batik sokaraja menggunakan sitem Fe_2O_3-H_2O_2-UV (Decrease level of methylene blue in Sokaraja liquid waste using Fe_2O_3-H_2O_2-UV system). Jurnal Rekayasa Kimia dan Lingkungan, 13, 78–86.

Ebelegi, A.N., Ayawei, N., &Wankasi, D. (2020). Interpretation of adsorption thermodynamics and kinetics. Open Journal of Physical Chemistry 10, 166–182. https://doi.org/10. 4236/ojpc.2020.103010

El-Bery, H.M., Saleh, M., El-Gendy, R.A., Saleh, M.R., Thabet, S.M., (2022). High adsorption capacity of phenol and methylene blue using activated carbon derived from lignocellulosic agriculture wastes. Scientific Reports, 12, 1–17. https://doi.org/10.1038/s41598-022-09475-4

El-Bindary, M.A., El-Desouky, M.G., & El-Bindary, A.A. (2022). Adsorption of industrial dye from aqueous solutions onto thermally treated green adsorbent: A complete batch system evaluation. Journal of Molecular Liquids, 346, 117082. https://doi.org/10.1016/j.molliq. 2021.117082

Esmaeili, H., & Foroutan, R. (2019). Adsorptive behavior of methylene blue onto sawdust of sour lemon, date palm, and eucalyptus as agricultural wastes. Journal of Dispersion Science and Technology, 40, 990–999. https://doi.org/10.1080/01932691.2018.148 9828

Etim, U.J., Umoren, S.A., & Eduok, U.M. (2016). Coconut coir dust as a low cost adsorbent for the removal of cationic dye from aqueous solution. Journal of Saudi Chemical Society, 20, S67–S76. https://doi.org/10.1016/j.jscs.

2012.09.014

Fatah, A.H., Agnestisia, R., Sciences, N., Raya, P., &Raya, P. (2022). Co-precipitation synthesis of clay-magnetite nanocomposite for adsorptive removal of synthetic dye in wastewater of benang bintik batik. *Molekul, 17* (2), 261–269.

Ganguly, P., Sarkhel, R., & Das, P. (2020). Synthesis of pyrolyzed biochar and its application for dye removal: Batch, kinetic and isotherm with linear and non-linear mathematical analysis. *Surfaces and Interfaces, 20,* 100616. https://doi.org/10.1016/j.surfin.2020.100616

Hameed, B.H., Mahmoud, D.K., & Ahmad, A.L. (2008). Equilibrium modeling and kinetic studies on the adsorption of basic dye by a low-cost adsorbent: Coconut (*Cocos nucifera*) bunch waste. *Journal of Hazardous Materials, 158,* 65–72. https://doi.org/10.1016/j.jhazmat.2008.01.034

Handayani, S.N., Irmanto, I., & Indriyani, N.N. (2023). Determination of the adsorption kinetics for adsorption methylene blue dye with C-4-hydroxy-3-methoxyphenylcalix[4] resorcinarene. *Molekul, 18,* 107–116.

Hasan, R., Ying, W.J., Cheng, C.C., Jaafar, N.F., Jusoh, R., Jalil, A.A., & Setiabudi, H.D. (2020). Methylene blue adsorption onto cockle shells-treated banana pith: Optimization, isotherm, kinetic, and thermodynamic studies. *Indonesian Journal of Chemistry, 20,* 368–378. https://doi.org/10.22146/ijc.42822

Hashemian, S., Ardakani, M.K., & Salehifar, H. (2013). Kinetics and thermodynamics of adsorption methylene blue onto Tea Waste/CuFe$_2$O$_4$composite. *American Journal of Analytical Chemistry, 4* (7A), 33865. https://doi.org/10.4236/ajac.2013.47A001

Hasti, F.S., Kopon, A.M., Baunsele, A.B., Tukan, M.B., Leba, M.A.U., Boelan, E.G., & Komisia, F. (2021). Identification of phytochemical extract of a combination of young coconut water, ginger and turmeric. *Indonesian Journal of Chemical Research, 9,* 129–136. https://doi.org/10.30598/ijcr

Huda, T., & Yulitaningtyas, T.K. (2018). Kajian adsorpsi methylene blue menggunakan selulosa dari alang-alang (Methylene blue adsorption study using cellulose from reeds). *Indonesian Journal of Chemical Analysis, 1,* 9–19. https://doi.org/10.20885/ijca.vol1.iss1.art2

Iriarte-Velasco, U., Sierra, I., Zudaire, L., & Ayastuy, J.L. (2016). Preparation of a porous biochar from the acid activation of pork bones. *Food and Bioproducts Processing, 98,* 341–353. https://doi.org/10.1016/j.fbp.2016.03.003

Jawad, N.H., & Najim, S.T. (2018). Removal of methylene blue by direct electrochemical oxidation method using a graphite anode. *IOP Conference Series: Materials Science and Engineering, 454,* 012023. https://doi.org/10.1088/1757-899X/454/1/012023

Jorge, N., Teixeira, A.R., Marchão, L., Tavares, P.B., Lucas, M.S., & Peres, J.A. (2022). Removal of methylene blue from aqueous solution by application of plant-based coagulants. *Engineering Proceedings,19*(1), 38. https://doi.org/10.3390/ECP2022-12659

Kamari, A., Yusoff, S.N.M., Abdullah, F., & Putra, W.P. (2014). Biosorptive removal of Cu(II), Ni(II) and Pb(II) ions from aqueous solutions using coconut dregs residue: Adsorption and characterisation studies. *Journal of Environmental Chemical Engineering, 2,* 1912–1919. https://doi.org/10.1016/j.jece.2014.08.014

Karić, N., Maia, A.S., Teodorović, A., Atanasova, N., Langergraber, G., Crini, G., Ribeiro, A.R.L., & Đolić, M. (2022). Bio-waste valorisation: Agricultural wastes as biosorbents for removal of (in)organic pollutants in wastewater treatment. *Chemical Engineering Journal Advances, 9,*100239. https://doi.org/10.1016/j.ceja.2021.100239

Khuluk, R.H., Rahmat, A., Buhani, & Suharso (2019). Removal of Methylene blue by adsorption onto activated carbon from coconut shell (*Cocous Nucifera* L.). *Indonesian Journal of Science and Technology, 4,* 229–240. https://doi.org/10.17509/ijost.v4i2.18179

Krishna Moorthy, A., Govindarajan Rathi, B., Shukla, S.P., Kumar, K., & Bharti, V. S (2021). Acute toxicity of textile dye Methylene blue on growth and metabolism of selected freshwater microalgae. *Environmental Toxicology and Pharmacology, 82,* 103552. https://doi.org/10.1016/j.etap.2020.103552

Kumar, M.S., N, S., E, D. (2019). Photocatalytic degradation of methylene blue using silver nanoparticles synthesized from gymnema sylvestre and antimicrobial assay. *Novel Research in Sciences, 2,* 1–7. https://doi.org/10.31031/nrs.2019.02.000532

Kusuma, H.S., Aigbe, U.O., Ukhurebor, K.E., Onyancha, R.B., Okundaye, B., Simbi, I., Ama, O.M., Darmokoesoemo, H., Widyaningrum, B.A., Osibote, O.A., Balogun, V.A., (2023). Biosorption of Methylene blue using clove leaves waste modified with sodium hydroxide. *Results in Chemistry, 5,* 100778. https://doi.org/10.1016/j.rechem.2023.100778

Lellis, B., Fávaro-Polonio, C.Z., Pamphile, J.A., & Polonio, J.C. (2019). Effects of textile dyes on health and the environment and bioremediation potential of living organisms. *Biotechnology Research and Innovation, 3,* 275–290. https://doi.org/10.1016/j.biori.

2019.09.001

Marković, S., Stanković, A., Lazarević, S., Stojanović, M., & Uskoković, D. (2015). Application of raw peach shell particles for removal of methylene blue. *Journal of Environmental Chemical Engineering, 3* (2) 716-724. https://doi.org/10.10 16/j.jece.2015.04.002

Mishra, Y., Sowmya, V., & Shanthakumar, S. (2015). Adsorption studies of basic dyes onto teak (*Tectona grandis*) leaf powder. *Journal of Urban and Environmental Engineering, 9*, 102–108. https://doi.org/10.4090/juee.2015.v9n2.102108

Nandhini, N.T., Rajeshkumar, S., & Mythili, S. (2019). The possible mechanism of eco-friendly synthesized nanoparticles on hazardous dyes degradation. *Biocatalysis and Agricultural Biotechnology, 19*, 101138. https://doi.org/10.1016/j.bcab.2019.101138

Neolaka, Y.A.B., Lawa, Y., Naat, J., Lalang, A.C., Widyaningrum, B.A., Ngasu, G.F., Niga, K.A., Darmokoesoemo, H., Iqbal, M., & Kusuma, H.S. (2023). Adsorption of methyl red from aqueous solution using Bali cow bones (*Bos javanicusdomesticus*) hydrochar powder. *Results in Engineering, 17,* 100824. https://doi.org/10.1016/j.rineng.2022.100824

Neolaka, Y.A.B., Lawa, Y., Naat, J.N., Riwu, A.A.P., & Iqbal, M., Darmokoesoemo, H., Kusuma, H.S. (2020). The adsorption of Cr(VI) from water samples using graphene oxide-magnetic (GO-Fe$_3$O$_4$) synthesized from natural cellulose-based graphite (kusambi wood or Schleicheraoleosa): Study of kinetics, isotherms and thermodynamics. *Journal of Materials Research and Technology, 9*, 6544–6556. https://doi.org/10.1016/j.jmrt.2020.04.040

Ninu, Y.D., & Baunsele, A.B. (2023). Study of methylene blue adsorption using siwalan fiber biosorbent activated by potassium hydroxide. *SPIN 5*, 50–66. https://doi.org/10.20414/spin.v5i1.6807

Nipa, S.T., Shefa, N.R., Parvin, S., Khatun, M.A., Alam, M.J., Chowdhury, S., Khan, M.A.R., Shawon, S.M.A.Z., Biswas, B.K., & Rahman, M.W. (2023). Adsorption of methylene blue on papaya bark fiber: Equilibrium, isotherm and kinetic perspectives. *Results in Engineering, 17*, 100857. https://doi.org/10.1016/j.rineng.2022.100857

Parushuram, N., Ranjana, R., Harisha, K.S., Shilpa, M., Narayana, B., Neelakandan, R., & Sangappa, Y. (2022). Silk fibroin and silk fibroin-gold nanoparticles nanocomposite films: sustainable adsorbents for methylene blue dye. *Journal of Dispersion Science and Technology, 43*, 1161–1176. https://doi.org/10.1080/01932691.2020.1848578

Pathania, D., Sharma, S., & Singh, P. (2017). Removal of methylene blue by adsorption onto activated carbon developed from *Ficus carica* bast. *Arabian Journal of Chemistry, 10*, S1445–S1451. https://doi.org/10.1016/j.arabjc.2013.04.021

Purnaningtyas, M.A.K., Sudiono, S., & Siswanta, D. (2020). Synthesis of activated carbon/chitosan/alginate beads powder as an adsorbent for methylene blue and methyl violet 2b dyes. *Indonesian Journal of Chemistry, 20*, 1119–1130. https://doi.org/10.22146/ijc.49026

Rangabhashiyam, S., Anu, N., & Selvaraju, N., 2013. Sequestration of dye from textile industry wastewater using agricultural waste products as adsorbents. *Journal of Environmental Chemical Engineering, 1*, 629–641. https://doi.org/10.1016/j.jece.2013.07.014

Salazar-Rabago, J.J., Leyva-Ramos, R., Rivera-Utrilla, J., Ocampo-Perez, R., & Cerino-Cordova, F.J. (2017). Biosorption mechanism of methylene blue from aqueous solution onto white pine (*Pinus durangensis*) sawdust: Effect of operating conditions. *Sustainable Environment Research, 27*, 32–40. https://doi.org/10.1016/j.serj.2016.11.009

Shakoor, M.B., Niazi, N.K., Bibi, I., Shahid, M., Sharif, F., Bashir, S., Shaheen, S.M., Wang, H., Tsang, D.C.W., Ok, Y.S., & Rinklebe, J. (2018). Arsenic removal by natural and chemically modified water melon rind in aqueous solutions and groundwater. *Science of the Total Environment, 645*, 1444–1455. https://doi.org/10.1016/j.scitotenv.2018.07.218

Sharma, S., Ezung, S.L., Supong, A., Baruah, M., Kumar, S., Umdor, R.S., & Sinha, D. (2023). Activated carbon adsorbent derived from waste biomass, "Croton caudatus" for efficient removal of 2-chlorophenol from aqueous solution: Kinetics, isotherm, thermodynamics and DFT simulation. *Chemical Engineering Research and Desig,n 190*, 777–792. https://doi.org/10.1016/j.cherd.2023.01.002

Silva, T.S., Meili, L., Carvalho, S.H. V., Soletti, J.I., Dotto, G.L., & Fonseca, E.J.S. (2017). Kinetics, isotherm, and thermodynamic studies of methylene blue adsorption from water by Mytella falcata waste. *Environmental Science and Pollution Research, 24*, 19927–19937. https://doi.org/10.1007/s11356-017-9645-6

Staroń, P., Chwastowski, J., & Banach, M., 2019. Sorption behavior of methylene blue from aqueous solution by raphia fibers. *International Journal of Environmental Science and Technology, 16*, 8449–8460. https://doi.org/10.1007/s13762-019-02446-9

Sulaeman, U., Ulumuddin, B.I., Andreas, R., Irmanto, I., & Iswanto, P. (2023). Adsorption of

Rhodamine B on spherical activated carbon synthesized from waste bagasse liquid using hydrothermal process. *Molekul 18* (1), 1–10. https://doi.org/10.20884/1.jm.2023.18.1.5510

Talaiekhozani, A., Reza Mosayebi, M., Fulazzaky, M.A., Eskandari, Z., & Sanayee, R. (2020). Combination of TiO_2 microreactor and electroflotation for organic pollutant removal from textile dyeing industry wastewater. *Alexandria Engineering Journal, 59*, 549–563. https://doi.org/10.1016/j.aej.2020.01.052

Umaningrum, D., Nurmasari, R., Santoso, U.T., Astuti, M.D., & Pradita, H.T. (2023). Adsorption of congo red onto humic acid isolated from peat soil gambut regency, South Kalimantan. *Molekul, 18*, 330–338.

Wulandari, A., Bahri, S., & Mappiratu, M. (2019). Antibacterial activity of ethanol extract of coconut coir (*Cocos nucifera* Linn) at various levels of aging. *Kovalen: Jurnal Riset Kimia, 4,* 276–284. https://doi.org/10.22487/kovalen.2018.v4.i3.11854

Xu, H., Zhang, P., Zhou, S.Y., & Jia, Q. (2020). Fullerene functionalized magnetic molecularly imprinted polymer: synthesis, characterization and application for efficient adsorption of methylene blue. *Chinese Journal of Analytical Chemistry, 48,* e20107–e20113. https://doi.org/10.1016/S1872-2040(20)60045-7

Yang, S., Wu, Y., Aierken, A., Zhang, M., Fang, P., Fan, Y., & Ming, Z. (2016). Mono/competitive adsorption of Arsenic(III) and Nickel(II) using modified green tea waste. *Journal of the Taiwan Institute of Chemical Engineers, 60*, 213–221. https://doi.org/10.1016/j.jtice.2015.07.007

Zhang, J., Amini, A., O'Neal, J.A., Boyer, T.H., & Zhang, Q. (2015). Development and validation of a novel modeling framework integrating ion exchange and resin regeneration for water treatment. *Water research, 84*, 255–265. https://doi.org/10.1016/j.watres.2015.07.027

Zuo, R., Du, G., Zhang, W., Liu, L., Liu, Y., Mei, L., & Li, Z. (2014). Photocatalytic degradation of methylene blue using TiO_2 impregnated diatomite. *Advances in Materials Science and Engineering, 2014*, 170148. https://doi.org/10.1155/2014/170148